Conference Paper

Nitrogen-Induced Modification of the Electronic Structure of Group III-N-V Alloys

Preprint

W. Walukiewicz, W. Shan, J.W. Ager III,
D.R. Chamberlin, and E.E. Haller
Lawrence Berkeley National Laboratory

J.F. Geisz, D.J. Friedman, J.M. Olson,
and S.R. Kurtz
National Renewable Energy Laboratory

*To be presented at the Electrochemical Society
International Symposium
Seattle, Washington
May 2-6, 1999*

NREL

National Renewable Energy Laboratory

NOTICE

Available electronically at http://www.doe.gov/bridge

Available for a processing fee to U.S. Department of Energy
and its contractors, in paper, from:
     U.S. Department of Energy
     Office of Scientific and Technical Information
     P.O. Box 62
     Oak Ridge, TN 37831-0062
     phone: 865.576.8401
     fax: 865.576.5728
     email: reports@adonis.osti.gov

Available for sale to the public, in paper, from:
     U.S. Department of Commerce
     National Technical Information Service
     5285 Port Royal Road
     Springfield, VA 22161
     phone: 800.553.6847
     fax: 703.605.6900
     email: orders@ntis.fedworld.gov
     online ordering: http://www.ntis.gov/ordering.htm

♻ Printed on paper containing at least 50% wastepaper, including 20% postconsumer waste

NITROGEN-INDUCED MODIFICATION OF THE ELECTRONIC STRUCTURE OF GROUP III-N-V ALLOYS

W. Walukiewicz, W. Shan, J. W. Ager III, D. R. Chamberlin and E. E. Haller,
Materials Sciences Division, Lawrence Berkeley National Laboratory, Berkeley,
California 94720

J. F. Geisz, D. J. Friedman, J. M. Olson and Sarah R. Kurtz
National Renewable Energy Laboratory, Golden, Colorado 80401

ABSTRACT

Incorporation of nitrogen in conventional III-V compound semiconductors to form III-N-V alloys leads to a splitting of the conduction band into two nonparabolic sub-bands. The splitting can be described in terms of an anticrossing interaction between a narrow band of localized nitrogen states and the extended conduction-band states of the semiconductor matrix. The downward shift of the lower sub-band edge is responsible for the N-induced reduction of the fundamental band-gap energy. The modification of the conduction-band structure profoundly affects the optical and electrical properties of the III-N-V alloys.

INTRODUCTION

It was discovered recently that replacement of group V elements with nitrogen leads to a dramatic change in the energy-band structure of the standard III-V compounds [1-4]. Incorporation of small concentrations of N into InGaAs results in a large (more than 180 meV per atomic % of N) decrease of the band gap [5]. This can be contrasted with the standard alloys where the change of the band gap is typically less than 10 meV per atomic % of any of the component elements. This discovery offers a new, independent way to control energy gaps and the conduction-band offsets in a large variety of III-V compounds for optoelectronic applications.

Previous theoretical attempts aimed at an understanding of this large red shift attributed it to large differences in the atomic size and electronegativities between group V elements like As or P and N atoms [6-11]. These attempts have met with only limited success because an accurate treatment of random alloys is very difficult within the existing band structure calculation methods. In this paper, we show that the effects of substitutional N on the band structure can be described in terms of a simple model of localized N states interacting with a band of extended states. The interaction splits the conduction band into two sub-bands and leads to large enhancement of the electron effective mass. The model explains many of the existing experimental results and predicts new effects that could be observed in the group III-N-V semiconductor alloys [12].

CONDUCTION-BAND STRUCTURE

We consider the group III-N-V alloys in which some of the column V elements are replaced by N atoms. It is now well established that an isolated N atom introduces a localized state with energy level E_N. In most III-V compounds, this level is located very close to the conduction band edge. It lies at about 0.25 eV above the conduction-band edge in GaAs and less than 0.1 eV below the conduction-band edge in GaP [13-15]. The fact that the level remains highly localized indicates that there is only weak hybridization between the orbitals of N atoms and the extended states, $E_M(k)$, of the semiconductor matrix. The existence of such states has been confirmed by theoretical calculations within the tight binding approximation framework [13,14].

Because of their highly localized nature, the N-states exhibit a much weaker pressure dependence compared to the delocalized conduction-band states. Therefore, external hydrostatic pressure can be used to change the location of the N-states relative to the conduction-band edge. Thus, a nitrogen level that is resonant with the conduction band in GaAs moves into the band gap at the pressure of about 2 GPa [15]. Similarly, the level moves into the band gap when GaAs is alloyed with GaP [13] or AlAs [16].

In considering the problem of group III-N-V alloys, we assume that N atoms substituted on the group V elements are randomly distributed in a crystal lattice and are only weakly coupled to the extended states of the host semiconductor matrix. The eigenvalue problem can then be written as

$$\begin{vmatrix} E-E_M(k) & -V_{NM} \\ -V_{NM} & E-E_N \end{vmatrix} = 0, \tag{1}$$

where $V_{NM} = \langle k|V|N \rangle$ is the matrix element describing the coupling between N-states and the extended conduction-band states, $V = \Sigma_s U(\mathbf{r}-\mathbf{R_s})$, and $U(\mathbf{r}-\mathbf{R_s})$ is the potential introduced by an N atom on a $\mathbf{R_s}$ site. The solution of Eq.(1) takes the form

$$E_\pm(k) = \{(E_N+E_M(k))\pm[(E_N-E_M(k))^2+4(V_{NM})^2]^{1/2}\}/2, \tag{2}$$

where the squared matrix-element coupling of k and N states is given by

$$|V_{NM}|^2 = \langle k|V|N \rangle \langle N|V|k \rangle$$

$$= \Sigma_s \Sigma_{s'} \iint V^{-2} d\mathbf{r} d\mathbf{r'} e^{i\mathbf{kr}} U^*(\mathbf{r}-\mathbf{R_s}) \Psi^*_N(\mathbf{r}-\mathbf{R_s}) U(\mathbf{r'}-\mathbf{R_{s'}}) \Psi_N(\mathbf{r'}-\mathbf{R_{s'}}) e^{-i\mathbf{kr'}}. \tag{3}$$

$\Psi_N(\mathbf{r})$ is the wavefunction of a N-state localized on the substitutional site. Eq.(3) is valid only for low N-concentrations when there is no appreciable overlap between functions $S(\mathbf{r}-\mathbf{R_s})=U(\mathbf{r}-\mathbf{R_s})\Psi_N(\mathbf{r}-\mathbf{R_s})$ located on different sites. Using Fourier transforms of the function $S(\mathbf{r})$, V_{NM} can be written as

$$|V_{NM}|^2 = |S(k)|^2 \{\Sigma_s \Sigma_{s'} \exp[i\mathbf{k}(\mathbf{R_s}-\mathbf{R_{s'}})]\}. \tag{4}$$

The double sum in Eq.(4) has to be averaged over all possible N-atom configurations in the host crystal lattice. For a random distribution, it equals the total number of substitutional N-atoms, which is proportional to the molar fraction of N in the alloys. In general, V_{MN} depends on the wavevector k through the k dependence of the Fourier transform $S(k)$. However, since we are interested in the k states close to the conduction-band edge only, we will assume that V_{NM} is independent of k. Therefore the matrix element describing the hybridization between N-states and the conduction-band states of the semiconductor matrix is given by:

$$V_{NM} = C_{NM}x^{1/2}, \qquad (5)$$

where C_{NM} is a constant dependent on the semiconductor matrix and x is the mole fraction of substitutional N.

Figure 1 shows an example of the calculated structure of two conduction sub-bands, $E_-(k)$ and $E_+(k)$. It is evident that the interaction with the dispersionless N-level results in highly nonparabolic-dispersion relations for the two sub-bands. The arrows show possible interband and inter-sub-band-optical transitions in such a system. The most striking prediction of the present model is the appearance of new optical transitions from the valence band to the upper sub-band edge. Such transitions were indeed observed
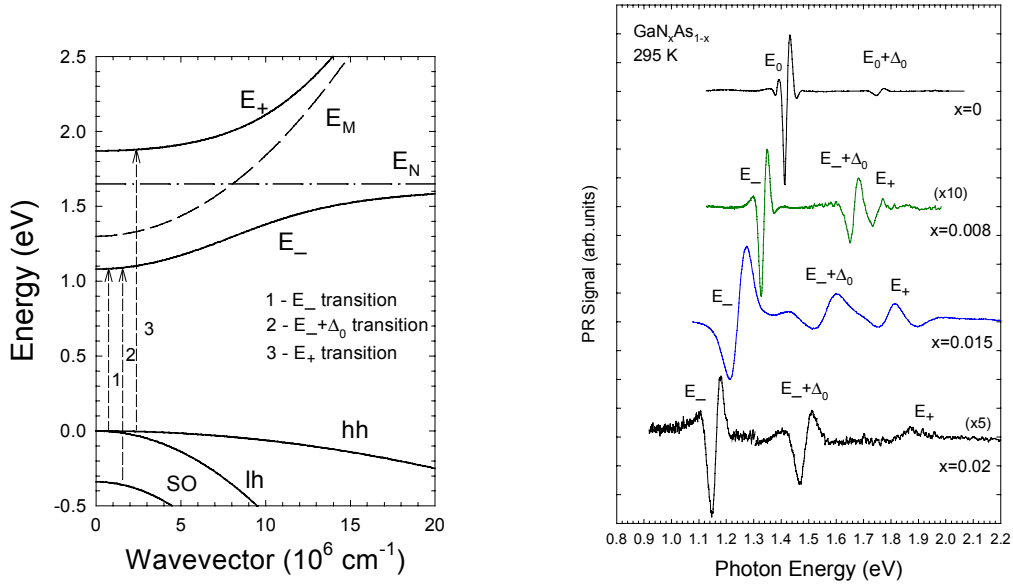

Figure 1. Dispersion curves for the lower and upper conduction sub-bands in GaNAs. E_M and E_N represent unperturbed conduction band of GaAs and the nitrogen level, respectively.
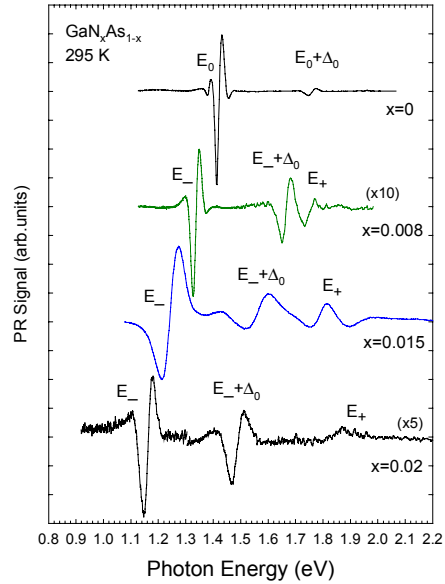
Figure 2. PR spectra of GaNAs recorded at room temperature.

using photomodulation spectroscopy [12,17]. Figure 2 shows photoreflectance (PR) spectra for a number of GaNAs samples. The transitions from the valence band to the lower and upper sub-band edges are clearly seen. As expected, the transitions to the lower sub-band shift to lower energy, while the transitions to upper sub-band shift to higher energy with increasing N-content.
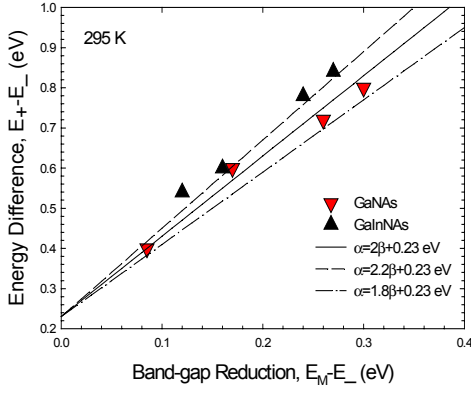
Figure 3. The relationship between the measured band splitting and band-gap shift for GaInNAs.

Using Eq.(2), one can obtain a simple relationship between the red shift of the band edge $\Delta E_G = E_M(k=0)-E_-(k=0)$ and the sub-band splitting $\Delta E=E_+-E_-$:

$$\Delta E = 2\Delta E_G + E_N-E_M(0). \qquad (6)$$

Because the location of the band edge of the host semiconductor matrix $E_M(0)$ is well known, one can use the relation given by Eq.(6) to determine the location of the N-level. Figure 3 shows the data for a number of GaInNAs samples. The experimental results follow quite closely the dependence predicted by Eq.(6), assuming that E_N is located at about 0.23 eV above the GaAs conduction-band edge or at 1.65 eV above the valence-band edge. This energy is in very good agreement with the position of the N-level previously found in lightly doped GaAs [15,16]. The results presented in Figure 3 indicate that incorporation of N predominantly affects the conduction band. The effect on the valence band is at least one order of magnitude smaller.
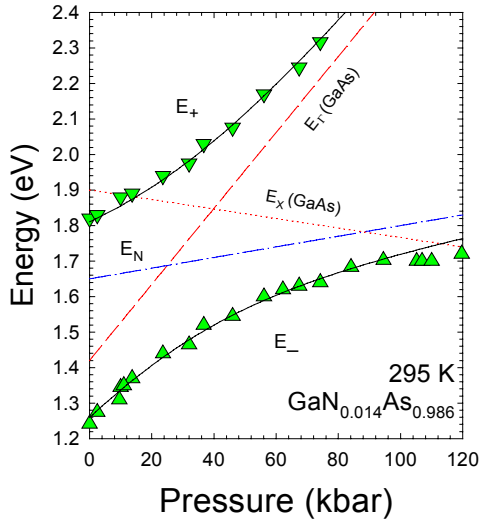

Figure 4. The effects of applied pressure on the E_- and $E+$ transition energies in $GaN_{0.015}As_{0.985}$.

Further support for our theory is provided by measurements of the energies of the sub-band edges as functions of hydrostatic pressure. Figure 4 shows the results of such measurements in $GaN_{0.015}As_{0.985}$. A characteristic anticrossing behavior is observed as the pressure changes the relative energies of E_N and $E_M(0)$. Using the known pressure derivatives ($dE_M/dP = 10.8$ meV/kbar and $dE_N/dP = 1.5$ meV/kbar), we can calculate the dependence of the sub-band edges on pressure. The calculations are in excellent agreement with the experimental results for $V_{MN}=0.2$ eV.

One of the important features of this new class of materials is the extraordinarily strong dependence of the band gap on the N-content. This dependence cannot be described in terms of standard models with a composition-independent-bowing parameter. The failure of this approach is understandable in view of our present results. The band gap is given by the energy of the lower sub-band edge $E_G=E_-(k=0)$. Substituting Eq.(5) into Eq.(2), one finds that in the small x limit when $2V_{NM}<<E_N-E_M(k=0)$, the red shift of the band edge is proportional to the N-content x and can be approximated by
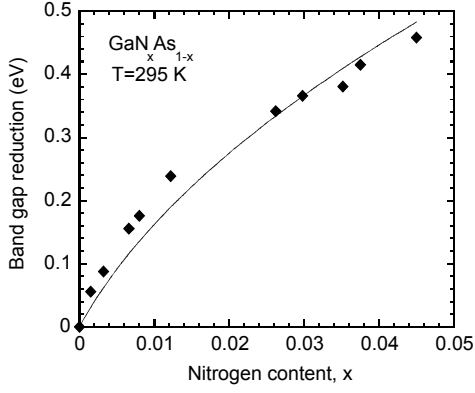
Figure 5. Dependence of the band gap reduction in GaN_xAs_{1-x} on the alloy composition. The line represents the best fit to Eq. (2) with $C_{NM}=2.7$ eV.

$$\Delta E_G = E_M(k=0) - E_-(k=0)$$
$$\approx (C_{NM})^2 x / (E_N-E_M). \qquad (7)$$

However, a weaker square-root dependence of ΔE_G on x is expected for larger x when $2V_{NM} \gg E_N-E_M(k=0)$.

The predicted dependence on the N-content is in a good agreement with the experiment. The experimental results on the recently re-evaluated N-induced reduction of the band gap in GaN_xAs_{1-x} [5] are shown in Figure 5. It is evident from the data that ΔE_G changes more rapidly for low x and tends to saturate at large x values. A very good fit to experimental data has been obtained using Eq.(2) with $C_{NM}=2.7$ eV. This, we believe, provides an accurate determination of the coupling constant for the GaAs matrix.

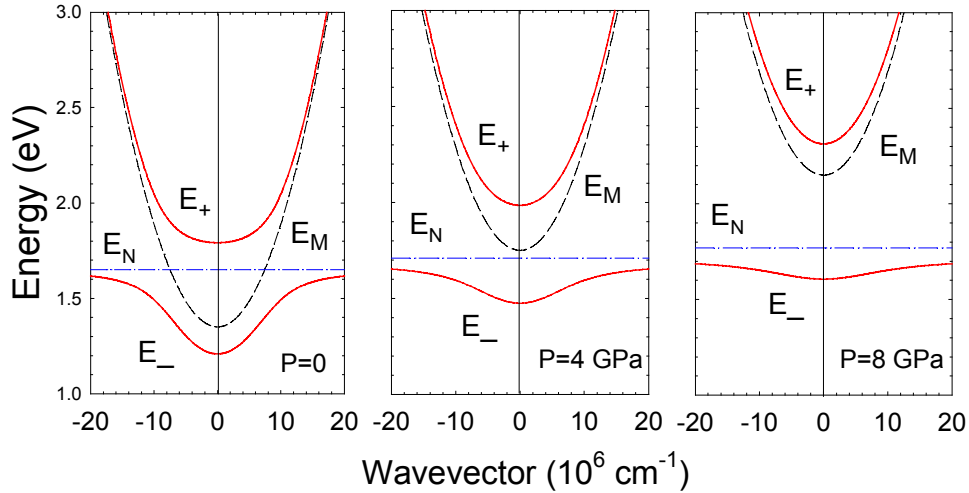So we have considered only the effect of the hybridization on the location of the sub-

Figure 6. The calculated dispersion of the E_- and E_+ sub-bands at three different pressures.

band edges. However it is clear from Figure 1 that the interaction has a dramatic effect on the dispersion relations $E_\pm(k)$ of the two conduction sub-bands. As the effect of the interaction is most pronounced for the states located close to E_N, it is not surprising that the dispersion relations for the conduction sub-bands are strongly affected by the pressure that shifts E_N with respect to the conduction band of the matrix. Figure 6 shows model calculations of $E_-(k)$ and $E_+(k)$ for three different values of hydrostatic pressure. The pressure has the strongest effect on the lower sub-band that narrows drastically at high
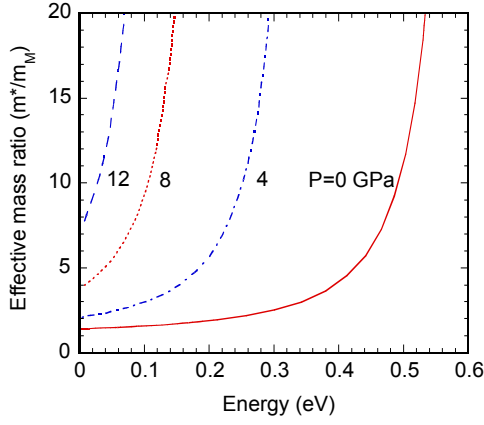
Figure 7. Dependence of the electron effective mass in the lower sub-band of $Ga_{0.92}In_{0.08}N_{0.02}As_{0.98}$ on the energy for different values of hydrostatic pressure. The effective mass of the GaInAs matrix $m_M=0.06m_0$.

pressures. Narrowing of the band indicates a gradual, pressure-induced transformation in the nature of the lowest sub-band from an extended to highly-localized state. This transformation can be also interpreted as a pressure-induced enhancement of the effective mass and the density of states in the lower sub-band.

We have calculated the electron effective mass as function of energy for different pressures using a standard definition of the density of states effective mass,

$$m_{eff} = (h/2\pi)^2 k(dE/dk)^{-1}. \tag{8}$$

Using Eqs.(2) and (8), one obtains a simple expression for the effective mass in the lower and upper sub-band,

$$m_{eff}(E)=m^*\{1+[V_{NM}/(E_N-E)]^2\}, \tag{9}$$

where m^* is the effective mass of the semiconductor matrix and E is the energy in the lower or upper sub-band measured from the valence-band edge. Eq.(9) reveals that the effective mass diverges for the electron energy approaching E_N. This is a result of the increasing contribution of the localized N-states to the electron states in the lower and upper sub-band.

The calculated effective masses for the case of $Ga_{0.92}In_{0.08}N_{0.02}As_{0.98}$ are shown in Figure 7. In the lower sub-band, we find a very large enhancement of the effective mass as a function of both electron energy and external pressure. An enhancement by almost two orders of magnitude is expected at high hydrostatic pressures. Because the effective mass of the corresponding $Ga_{0.92}In_{0.08}As$ matrix equals $0.06m_0$, the predicted mass can be larger than the free electron mass, m_0 in this case. A large enhancement of the electron-effective mass has been recently observed in magneto-photoluminescence experiments [18]. The enhancement of the effective mass leads to a very large density of states in the lower sub-band. This, as we will show below, has a profound effect on transport properties of electrons in the group III-N-V alloys.

ELECTRON TRANSPORT

The massive N-induced modifications of the conduction band structure is expected to affect electron transport properties of the III-N-V alloys. However, because the interaction is almost exclusively limited to the conduction band, we do not expect any significant effects of the N on the hole transport in the valence band. These expectations are confirmed by measurements of electron and hole mobilities in n- and p-type GaInNAs alloys. Recent reports indicate that in unintentionally doped samples, room temperature

hole mobilities can be as high as 200 cm^2/Vs [19]. Such mobilities are close to what is expected for standard III-V compounds with the hole effective mass of about 0.5m$_0$. On the other hand, measured electron mobilities are typically only of the order of a few hundred cm^2/Vs. These mobilities are significantly lower than typical electron mobilities observed in III-V compounds and their alloys. Thus, in GaAs with an electron effective mass of 0.067m$_0$, mobilities of several thousand cm^2/Vs are typically observed for electron concentrations below 10^{18} cm^{-3} [20]. Similar, or even slightly higher, electron mobilities are found in GaInAs alloys with a small In content.

A simple way to describe the effect of N on the electron mobility is to consider scattering of electrons by the potential difference between an anion atom of the semiconductor matrix and the randomly distributed substitutional N-atom. The microscopic, energy dependent electron mobility for the electrons in the lower sub-band can be then written as:

$$\mu_{ad}=(h^3e)/(8\pi^2m_{eff}^2k|V_{ad}|^2\Omega x), \tag{10}$$

where Ω is the volume of the unit cell, m$_{eff}$ is the energy dependent effective mass given by Eq.(9), and k is the wavevector that, according to Eq.(2), can be written as,

$$k=2\pi\{2m^*[(E-E_M)(E_N-E)+|V_{NM}|^2]/(E_N-E)\}^{1/2}/h. \tag{11}$$

The parameter describing the strength of the scattering is given by:

$$V_{ad}=d\Delta E_c/dx=|C_{NM}|^2/[(E_N-E_M(k))^2+4|C_{NM}|^2x]^{1/2}, \tag{12}$$

where $\Delta E_c(x)$ represents the N-induced shift of the conduction band edge. There are two factors that contribute to the reduction of electron mobility in GaInNAs. Firstly, for small x, the scattering parameter V$_{ad}$ can be as large 20 to 30 eV. This results in alloy disorder scattering that is almost 3 orders of magnitude more efficient than the scattering in standard semiconductor alloys, where V$_{ad}$ is typically smaller than 1 eV. Secondly, it is important to note that the mobility given by Eq.(10) is strongly dependent on the effective mass. Because, as it has been discussed above, the incorporation of N leads to a considerable enhancement of the effective mass, this will result in an additional reduction of the electron mobility. An electron mobility of about 500 cm^2/Vs has been calculated for GaN$_x$As$_{1-x}$ with x=0.01 and electron concentration of 3×10^{17} cm^{-3}.

MAXIMUM DOPING OF III-N-V ALLOYS

Ability to control the concentration of free carriers through doping is one of most important characteristics of semiconductor materials. Practical applications of many semiconductor materials are severely hampered by limitations on the maximum achievable electron and/or hole concentration. A universal rule to predict the maximum carrier concentration that can be achieved by doping has been proposed and successfully applied to variety of semiconductor materials [20-22]. The rule is based on the Amphoteric Native Defect (AND) model that relates the type and concentrations of native defects responsible for the compensation to the location of the Fermi level with respect to the common energy reference, Fermi level stabilization energy, EFS.

Semiconductor materials with the conduction (valence) band located close to E_{FS} can be easily doped n-type (p-type). Thus, GaAs with the conduction band at E_{FS}+0.9 eV and the valence band at E_{FS}-0.5 eV, exhibits strict limitations on the maximum free electron concentration but can be doped quite heavily p-type.

The large effect of nitrogen on the conduction band raised the interesting question whether III-N-V materials should exhibit higher n-type doping limits. As shown Figure 5, a downward shift of the conduction band by as much as 0.5 eV is observed in GaN_xAs_{1-x} with x=0.05. In GaAs, the maximum electron concentration achievable under equilibrium condition is limited to about 5×10^{18} cm^{-3}. This concentration corresponds to the Fermi energy located approximately at 0.1 eV above the conduction band edge or at 1 eV above E_{FS}. According to the Amphoteric Defect Model, this maximum location of the Fermi energy, relative to E_{FS}, is approximately constant for all group III-V semiconductors. Therefore, in GaN_xAs_{1-x}, the maximum Fermi energy position measured with respect to condition band edge increases rapidly with increasing N-content and can be as large E_c+0.6 eV for x=0.05. This should lead to largely improved activation of donors in the III-N-V alloys. A further increase in the maximum electron concentration originates from an enhancement of the electron effective mass, and thus, also the density of states in the conduction band of GaN_xAs_{1-x} alloys.
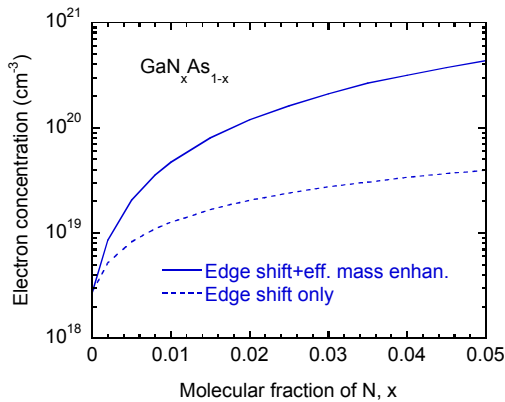

Figure 8. Calculated maximum electron concentration vs. nitrogen fraction in GaN_xAs_{1-x} .for two different cases that include effects of the downward shift of the conduction band edge only (dashed curve), and both the conduction band shift and the enhancement of the density of states effective mass (solid curve).

Figure 8 shows the calculated maximum electron concentration as function of the N-mole fraction for GaN_xAs_{1-x}. The dashed curve represents the case when only the downward shift of the conduction band is taken into account. A more than order of magnitude enhancement of the maximum electron concentration is predicted for x=0.05 in this case. Also, as is shown in Figure 8 (solid curve), an enhancement of the maximum electron concentration by more than two orders of magnitude is expected when the effects of both band-edge shift and the effective-mass enhancement are included in the calculations. There is only a very limited amount of data on n-type doping of group III-N-V alloys. Recent results on Se doping indicate that, indeed, a very large enhancement of the maximum n-type doping levels can be achieved in III-N-V alloys. $Ga_{0.95}In_{0.05}N_{0.022}As_{0.978}$ grown by MOCVD with DESe as a Se source have shown electron concentrations ranging from about 2×10^{19} to 5×10^{19} cm^{-3}, with corresponding electron mobilities in the range 100 to 40 cm^2/Vs. These electron concentrations are at least several times larger than what could be achieved in GaAs or $Ga_{0.95}In_{0.05}As$ under similar growth conditions. Because these large improvements of the maximum doping were achieved in an alloy with only 2.2% of

N shows that the maximum doping level is determined by the modification of the conduction band, rather than changes in chemical composition of the alloy.

CONCLUSIONS

We have shown that the interaction between highly localized N-levels and the extended states of the semiconductor matrix leads to a significant modification of the conduction-band structure of III-N-V alloys. The interaction splits the conduction band into two nonparabolic sub-bands with energy dependent effective masses. The downward shift of the lower sub-band fully explains the N-induced reduction of the energy gap. We show that the modification of the conduction-band structure profoundly affects the optical and electrical properties of the III-N-V alloys.

ACKNOWLEDGEMENTS

REFERENCES

1. M. Weyers, M. Sato, H. Ando, Jpn. J. Appl. Phys. **31**, L853 (1992).
2. J. N. Baillargeon, K. Y. Cheng, G. F. Hofler, P. J. Pearah and K. C. Hsieh, Appl. Phys. Lett., **60**, 2540 (1992).
3. M. Kondow, K. Uomi, K. Hosomi and T. Mozume, Jpn. J. Appl. Phys., **33**, L1056 (1994).
4. W. G. Bi, and C. W. Tu, J. Appl. Phys., **80**, 1934 (1996).
5. K. Uesugi, N. Marooka and I. Suemune, Appl. Phys. Lett., **74**, 1254 (1999).
6. J. A. Van Vechten, Phys. Rev., **182**, 891 (1969).
7. J. A. Van Vechten, Phys. Rev., **187**, 1007 (1969).
8. A. Rubio and M. L. Cohen, Phys. Rev., **B51**, 4343 (1995).
9. J. Neugebauer and C. G. Van de Walle, Phys. Rev., **B51**, 10568 (1995).
10. S.-H. Wei and A. Zunger, Phys Rev. Lett., **76**, 664 (1996).
11. L.-W. Wang, L. Bellaiche, S. –H. Wei and A Zunger, Phys. Rev. Lett., **80**, 4725 (1998).
12. W. Shan, W. Walukiewicz, J. W. Ager III, E. E. Haller, J. F. Geisz, D. J. Friedman, J. M. Olson and Sarah R. Kurtz, Phys. Rev. Lett., **82**, 1221 (1999).
13. H. P. Hjalmarson, P. Vogl, D. J. Wolford and J. D. Dow, Phys. Rev. Lett., **44**, 810 (1980).
14. S. Y. Ren, J. D. Dow and D. J. Wolford, Phys., Rev. **B25**, 7661 (1982).
15. X. Liu, M. E. Pistol, L Samuelson, S. Schwetlick and W. Seifert, Appl. Phys. Lett., **56**, 1451 (1990).
16. Y. Makita, H. Ijuin and S. Gonda, Appl. Phys. Lett., **28**, 287 (1976).
17. J. D. Perkins, A. Mascarenhas, Y. Zhang, J. F. Geisz, D. J. Friedman, J. M. Olson and S. R. Kurtz, Phys. Rev. Lett., **82**, 3312 (1999).

18. W. Walukiewicz, J. Lagowski, L. Jastrzebski, M. Lichtensteiger and H. C. Gatos, J. Appl. Phys., **50**, 899 (1979).
19. J. F. Geisz, D. J. Friedman, J. M. Olson, Sarah R. Kurtz and B. M. Keyes, J. Cryst. Growth, **195**, 401 (1998).
20. W. Walukiewicz, Appl. Phys. Lett., **54**, 2094 (1989).
21. W. Walukiewicz, Mat. Res. Soc. Symp. Proc., vol **300**, p 421 (1993).
22. S. B. Zhang, Su-Huai Wei, and A. Zunger, J. Appl. Phys. **83**, 3192 (1998).